Journal of Applied Polymer Science

Preparation and characterization of braided tube reinforced polyacrylonitrile hollow fiber membranes

Quan Quan,[1,2] Changfa Xiao,[1,2] Hailiang Liu,[2] Qinglin Huang,[2] Wei Zhao,[2] Xiaoyu Hu,[2] Guolan Huan[2]

[1]School of Textile, Tianjin Polytechnic University, Tianjin 300387, People's Republic of China

[2]State Key Laboratory of Hollow Fibre Membrane Materials and Processes, Tianjin Polytechnic University, Tianjin 300387, People's Republic of China

Correspondence to: C. Xiao (E-mail: xiaochangfa@163.com)

ABSTRACT: Polyacrylonitrile (PAN) and polyester (PET) braided hollow tube that used as a special reinforcement are braided from their filaments via two-dimensional weaving techniques. PAN braided tube reinforced homogeneous PAN hollow fiber membranes and PET braided tube reinforced heterogeneous PAN hollow fiber membranes are prepared by concentric circles squeezed-coated spinning method. As for PAN hollow fiber membrane, the effects of PAN concentration on the performance of the prepared hollow fiber membranes are investigated in terms of pure water flux, protein rejection, mechanical strength, and morphology observations by a scanning electron microscope (SEM). The interfacial bonding state of the braided tube reinforced PAN hollow fiber membranes is studied by constant speed stretching method. Results show that the breaking strength of two-dimensional braided tube reinforced PAN hollow fiber membranes is higher than 80 MPa. The structure of separation surface is similar to the structure of an asymmetric membrane. With the increase of polymer concentration, the membrane flux decreases while the retention rate of BSA increase. The membrane porosity and maximum pore size have the same decreasing tendency as the increase of PAN concentration. The results also show that the interfacial bonding state of the PAN two-dimensional braided tube reinforced homogeneous PAN hollow fiber membranes is better than that of the PET two-dimensional braided tube reinforced heterogeneous PAN hollow fiber membranes.
 J. Appl. Polym. Sci. **2015**, *132*, 41795.

KEYWORDS: mechanical properties; membranes; properties and characterization; separation techniques; surfaces and interfaces

Received 27 July 2014; accepted 22 November 2014

DOI: 10.1002/app.41795

INTRODUCTION

Recently, the environmental problems have become a critical issue. Membrane separation technologies such as ultra-filtration (UF) and microfiltration (MF) have been wildly applied to deal with various manufacturing industries wastewater treatment.[1,2] Nowadays, the most popularly used UF and MF hollow fiber membranes that consisted of skin layer and support layer, are usually prepared through the immersion phase inversion method. It usually turns out to be a typical structure of asymmetric membrane which shows a dense skin layer and porous support layer.[3] The support layer in which includes pores and micro pores is dominated by many variables such as polymer concentration,[4] coagulation temperature,[5] solvent and non solvent composition,[6] organic and inorganic additives.[7–9] The hollow fiber membranes are mechanical self-supporting and easy to assemble in modules which are attractive for industrial application. And such membranes have been broadly applied in membrane bioreactor (MBR) systems.[10] The MBR has emerged as an attractive technology for advanced municipal and industrial wastewater treatment, and offers lots of advantages over conventional wastewater treatment processes, including low sludge production, excellent quality effluent and reduced footprint.[11,12] However, the hollow fiber membranes are liable to be damaged or broke by the high-pressure cleaning process or disturbance of the aerated airflow during the MBR process. In the application of such water treatment, the membranes are demanded not only for theirs being preeminent in separation and permeation performance but for theirs excellent mechanical property.[13,14]

Several researches have studied on how to improve the mechanical strength of hollow fiber membranes. A fabric, tubular braid, or threads are used for reinforcing and supporting the hollow fiber membrane owing to their excellent mechanical strength. Lee *et al.*[15] has invented a braid-reinforced hollow fiber membrane that contains a reinforcement tubular braid and a polymer resinous thin film coated on the surface of the reinforcement tubular braid. The preparation of PET threads reinforced polyvinylidene fluoride (PVDF) hollow fiber membranes was researched by Liu *et al.*[16] It was found that the tensile/rupture strength of the

threads reinforced membranes were remarkably improved to 10 MPa. However, this kind of hollow fiber membrane had problems that the interfacial bonding state was weak and the surface layer was easily peeled from the reinforcement due to the surface layer and reinforcement were thermodynamic incompatible. Therefore, prepared a homogeneous reinforced hollow fiber membrane, in which the surface layer and the reinforced layer are the same materials, could ameliorate the interfacial bonding state. Zhang *et al.*[17] have researched the preparation and properties of HR PVDF hollow fiber membrane. They found that the HR PVDF hollow fiber membrane had a favorable interfacial bonding between the surface coating layer and the matrix membrane.

Polyacrylonitrile (PAN) is a superior polymeric materials for making membrane.[18] PAN hollow fiber membranes have been widely used in the treatment of industrial wastewater treatment,[19] pervaporation process,[20] enzyme immobilization,[21] biomedical applications,[22] and fabrication of the substrate of composite membranes,[23,24] due to its low price, excellent ageing-resisting property and other advantages. However, its low mechanical endurance limits its application in UF or MF dealing with evil wastewater, especially, for the MBR systems.

In this study, hollow fiber membranes that included a PAN casting solution that as the coating layer and the two-dimensional braided tube which had an excellent mechanical strength as a support matrix for the separation membrane were prepared through the dry-wet spinning process, based on the theory of thermodynamic compatibility and the technology of skin-core composite spinning of chemical fiber. The process was named the two-dimensional braid reinforced (BR) method. The PAN two-dimensional braided tube reinforced homogeneous PAN hollow fiber membranes (PAN BR) and polyester (PET) two-dimensional braided tube reinforced heterogeneous PAN hollow fiber membranes (PET BR) were prepared by the BR method. The mechanical properties of the BR membranes and the influences of the PAN concentration in the polymer solutions on the membrane structure and permeability were studied. Furthermore, the interfacial bonding state between the surface separation layer and the two-dimensional braided matrix was investigated.

EXPERIMENTAL

Materials

PAN, 150 D/60F and PET 150 D/96F filaments were supplied by Xiangying Special Fibre (Changshu, China) and Sinopec Yizheng Chemical Fibre (Yizheng, China), respectively. PAN (molecular weight 50,000) was purchased from the Qilu Petrochemical Acrylic Factory. *N*,*N*-Dimethylacetimide (DMAc, Analytical Reagent, $>99\%$) and polyvinylpyrrolidone (PVP, K30, Analytical Reagent, $M_w = 30{,}000$) were obtained from Tiantai Fine Chemical (Tianjin, China). Tween 80 (Tw-80, Analytical Reagent) was purchased from Tianjin Fengchuan Chemical Reagent Science and Technology (Tianjin, China).

Preparation of Braided Tube Reinforced PAN Hollow Fiber Membranes

The PAN and PET filaments were braided into a two-dimensional hollow tubular braid as the reinforced matrix via two-dimensional braid technology, respectively. The two-dimensional braid was cleaned by neutral liquid abstergent for removing the oiling agent which coated on the chemical filaments surface during spinning process, then dried at 25°C and winded for next process. Figure 1 shows the surface SEM morphologies of the two-dimensional braid, which surface exhibited a similar rhombus structure and was possessed of a number of gaps between the filaments.

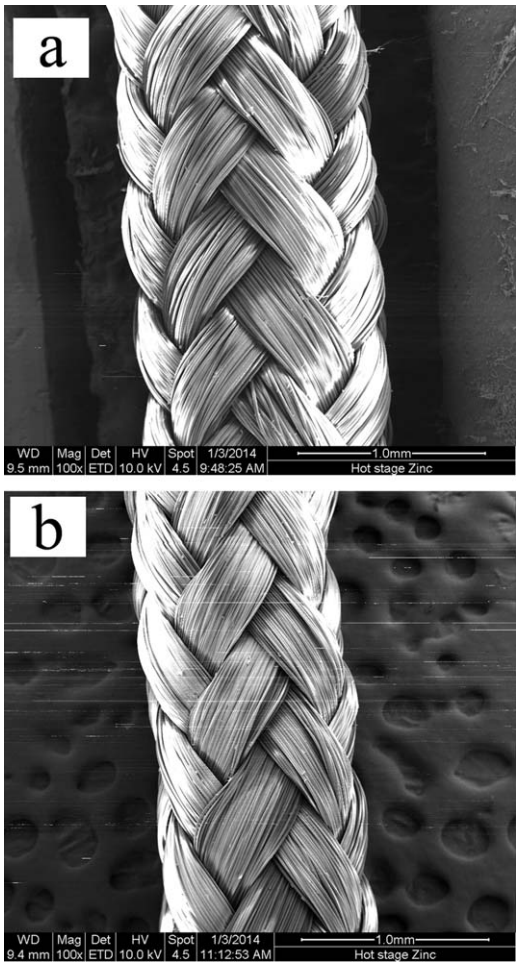

Figure 1. Surface structure of the two-dimensional braid tube: (a) PAN; (b) PET.

The reinforced PAN hollow fiber membranes were prepared by the dry–wet spinning BR method. Figure 2 shows the spinning apparatus. The traction of the winding device made the filaments braided into a tubular two-dimensional fabric such as a hollow fiber, during the two-dimensional braiding process. The different systems filaments were braided each other, and produced a lot of gaps between the filaments, showed in Figure 1. Therefore, some of the polymer solutions could infiltrate into the gaps in the membrane spinning process, which improved the interfacial bonding between surface separation layer and the two-dimensional braid matrix. According to the method described, the PAN (or PET) two-dimensional braid tube were coated with the polymer solutions and guided through a coagulation bath. After being immersed in deionized water for 48 h, the polymer solutions were converted into a microporous layer

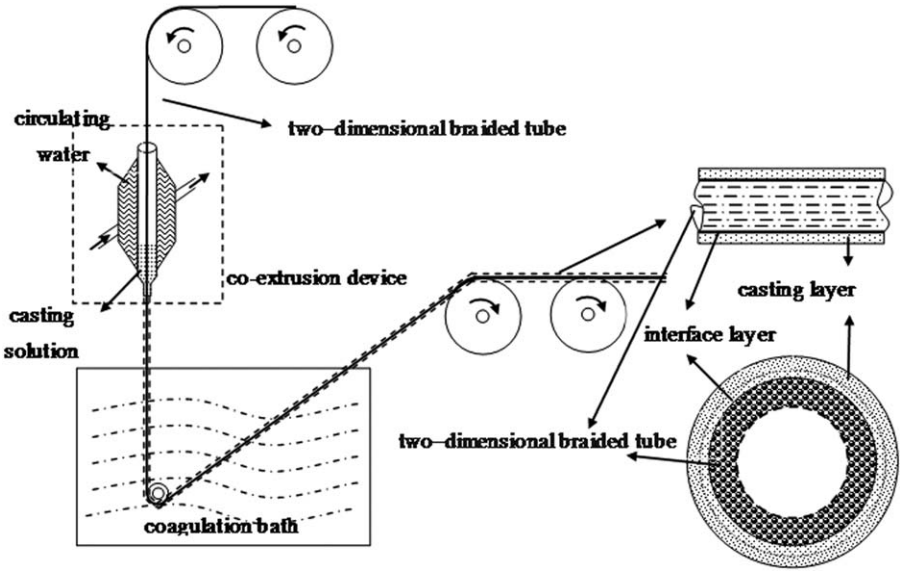

Figure 2. Schematic diagram describing of the two-dimensional braided tube reinforced PAN membrane.

and some of the polymer solutions were embedded within the gaps of the two-dimensional braid tube.

The polymer solutions were prepared by the blending of different compositions consisting of PAN, PVP K30, Tw-80, and DMAc, showed in Table I, under constant mechanical stirring in a three-necked round-bottom flask for 4 h at 70°C. All the membranes were prepared under the temperature of 25°C and at the environmental humidity of 60%. The PAN BR membranes with the different PAN concentrations, i.e., 10, 12, 14, 16, and 18 weight (wt %) were labeled M10, M12, M14 M16, and M18, respectively. The PET BR membranes with the different PAN concentrations, i.e., 10, 12, 14, 16, and 18 weight (wt %) were labeled N10, N12, N14 N16, and N18, respectively. Before the scanning electron microscope (SEM) tests, we put the resulting membranes in glycerol water solutions (a half glycerol to a half water) and then dried them in air, so as to retain the porous structure.

Membrane Characterizations

Mechanical Strength Testing. The tensile strength and elongation at break of the hollow fiber membranes were determined at room temperature by using a JBDL-200 electronic tensile testing machine (Yangzhou, China). The tensile speed rate was 20 mm min^{-1} and the clamping length was 100 mm.

Table I. Spinning Parameters of PAN Membranes with Different Dope Composition

PAN BR	PET BR	PAN (wt %)	PVP (wt %)	Tw-80 (wt %)	DMAc (wt %)
M10	N10	10	7	2	81
M12	N12	12	7	2	79
M14	N14	14	7	2	77
M16	N16	16	7	2	75
M18	N18	18	7	2	73
Dope solution temperature (°C)			70		
Extra coagulation Water (°C)			25		
Air gap (cm)			15		
Take up speed (cm min^{-1})			20		

Morphology Examination. The morphology of the membranes was observed using a scanning electron microscope (SEM), (Quanta200, FEI, Czech). The samples were lyophilized, followed by fracturing to expose their cross-sectional areas and surface. Thereafter, they were sputtered with gold and observed through SEM.

Membrane Permeability. The pure water flux (PWF) of the membranes was determined using eq. (1). The pressure difference across the membrane was 0.1 MPa under the condition of outside feeding. The membrane module contained three hollow fiber membranes with an effective area of 1.23×10^{-6} m^2.

$$J = \frac{V}{S \times t} \quad (1)$$

where J is the PWF (L m^{-2} h^{-1}), V is the quantity of the permeate (L), S is the membrane area (m^2), and t is the testing time (h).

The filtration experiments were carried out using the protein solution. The rejection of the membranes was measured with 1.0 g L^{-1} bovine serum albumin (BSA, $M_w = 68{,}000$) solution and calculated using eq. (2).

$$R(\%) = \left(\frac{C_f - C_p}{C_f}\right) \times 100\% \quad (2)$$

where C_p and C_f are the concentration at permeate and feed, respectively.

Each membrane module was initially pressurized for 20 min at 0.15 MPa. The pressure was then reduced to the operating pressure of 0.1 MPa, and the PWF was measured. Before the protein filtration, the membranes were compacted at 0.1 MPa for 60 min, then, the rejection was measured at 0.1 MPa.

Membrane Porosity Determination. The membrane porosity (ε) was defined as the pores volume divided by the total volume of the porous membrane. It was calculated according to eq. (3).

Table II. The Contact Angle between the Two-Dimensional Braid Matrix and the Casting Solution

Two-dimensional braid tube	PAN concentration (wt %)				
	10	12	14	16	18
PAN	70.4° ± 0.2°	71.6° ± 0.1°	72.3° ± 0.2°	75.1° ± 0.1°	79.3° ± 0.2°
PET	75.4° ± 0.2°	77.2° ± 0.1°	78.7° ± 0.3°	81.5° ± 0.2°	83.4° ± 0.3°

$$\varepsilon = \frac{w_1 - w_2/\rho_1}{w_1 - w_2/\rho_1 + w_2 - w_3/\rho_2 + w_3/\rho_3} \times 100\%, \quad (3)$$

where W_1 and W_2 are the weights of the wet and the dry membranes, respectively, W_3 is the weight of the two-dimensional braid, ρ_1 is the water density, ρ_2 is the polymer density (1.15 g cm^{-3}), and ρ_3 is the two-dimensional braid density (PAN, 1.15 g cm^{-3}; PET, 1.38 g cm^{-3}).

Maximum Pore Size of the Membrane. The maximum pore size of the membranes was obtained using the bubble point method with alcohol as wetting liquid and calculated using eq. (4).

$$r_p = \frac{2\gamma}{P} \quad (4)$$

where r_p is the maximum pore size of the membrane (μm), γ is the surface tension at the alcohol/air interface (N m^{-1}), and P is the pressure. At room temperature (20°C), γ is equal to 22.32 × 10^{-3} N m^{-1}.

Interfacial Bonding State of the Reinforced PAN Membranes. The interfacial bonding state of the two-dimensional braided tube reinforced PAN hollow fiber membrane was determined by constant speed stretching method. After stretching, the interfacial bonding state was investigated by terms of pure water flux, protein rejection, and morphology observations by SEM, indirectly. The constant speed stretching determined at room temperature by a JBDL-200 electronic tensile testing machine (Yangzhou, China). The stretch speed rate was 20 mm min^{-1}, the clamping length was 300 mm, and the set-stretching time was 30 min.

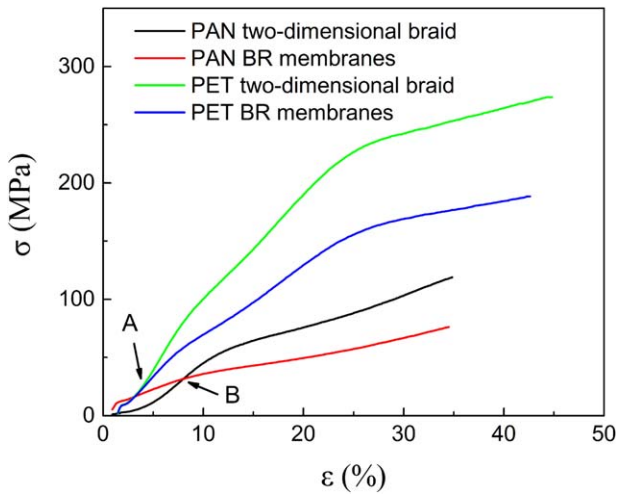

Figure 3. The mechanical properties of the two-dimensional braid and reinforced hollow fiber membranes. [Color figure can be viewed in the online issue, which is available at wileyonlinelibrary.com.]

RESULTS AND DISCUSSIONS

Infiltration Properties of the Polymer Solutions

Normally, one phase contacted with the other phase of the solution or melt states in the two phases of the composite materials, and then combined with the curing reaction. The adhesion action referred to the state in which the two surfaces were combined with the chemical or physical interaction.[25] The infiltration between the polymer solutions and the two-dimensional braid matrix will influence the interface. Poor infiltration leaded to defects or stress concentration near the interface, therefore, the interfacial bonding state weakened; conversely, favorable infiltration could ameliorate greatly on the interfacial bonding state. The infiltration ability was characterized by the contact angle measurement. Smaller contact angle between the polymer solutions and the two-dimensional braid matrix, the better infiltration and contacting between them. The contact angle between the polymer solutions and the two-dimensional braid matrix was showed in Table II, in which average of the five samples, the temperature of PAN casting solutions was 70°C and the contacting time was 5 s. With the increase of PAN concentration, the contact angles of the PAN and PET two-dimensional braid matrix increased gradually, but were <90°. This was due to the polymer solution viscosity increased with the increase of PAN concentration, so the fluidity of the solution was weakened. In addition, the two-dimensional braid matrix was possessed of numerous gaps as shown in Figure 1, which were much larger than the size of macromolecules in the casting solution. Wherefore the casting solution infiltrated into the two-dimensional braid matrix and improved the interfacial bonding state. The contact angle between the PAN casting solutions and the two-dimensional braid matrix was lesser than that of the PET at the same PAN concentration. The reason is that the PAN casting solutions and the PAN two-dimensional braid were thermodynamic compatibility and the DMAc in the PAN casting solutions was excellent co-solvent of them, but the PAN casting solutions and the PET two-dimensional braid were thermodynamic incompatibility and DMAc was not co-solvent of them. Thus the infiltration and contact between the PAN casting solutions and the PAN two-dimensional braid matrix were better than that of the PAN casting solutions and the PET two-dimensional braid matrix.

Tensile Strength of the Hollow Fiber Membranes

Figure 3 shows the stress–strain curves of the PAN and PET two-dimensional braid and their reinforced PAN membranes, respectively. Table III shows the mechanical data of the two-dimensional braid and reinforced hollow fiber membranes.

Table III. The Mechanical Data of the Two-Dimensional Braid and Reinforced Hollow Fibre Membranes

	Yield strength (MPa)	Young's modulus (MPa)	Breaking strength (MPa)	Breaking elongation (%)
PET braid	226.7 ± 4.5	1198.6 ± 10.5	275.0 ± 4.5	45.2 ± 1.8
N12	150.0 ± 2.5	705.4 ± 8.0	188.0 ± 2.0	42.2 ± 0.8
PAN braid	62.5 ± 1.8	366.8 ± 2.4	120.0 ± 4.0	35.8 ± 1.2
M12	31.2 ± 0.2	323.8 ± 0.6	86.3 ± 1.2	33.8 ± 0.8

Figure 3 displays that the tensile strength of the PET two-dimensional and PET BR membranes was different from the PAN two-dimensional braid and PAN BR membranes. The stress–strain curves of the PET two-dimensional braid and PET BR membranes were overlap in the initial stages of the tensile. When the PET two-dimensional braid and PET BR membranes were stretched in the infancy, there was only a small tension could make the rhombus structure of the two-dimensional braid produced a greater tensile deformation. Before A point in the curves, a little stress and large tensile strain were displayed as shown in Figure 3. At this range, with the increase of the tensile strength, the rhombus structure deformation took place and the braided angle decreased. However, the rhombus structure deformation could be reversion to previous state if removed the tension. After A point, the rhombus structure deformation increased sharply and became irreversible with the increase of tension. The tensile curves of the PAN two-dimensional braid and PAN BR membranes were very distinct, curve of the PAN BR membranes was higher than the PAN two-dimensional braid before B point, but it was lesser than the PAN two-dimensional braid after the B point. Table III displays that the yield strength, young's modulus, breaking strength and breaking elongation of the BR hollow fiber membrane were smaller than that of the two-dimensional braid, severally. These phenomena occurred because the polymer solution were not only coated on the surface uniformly, but also infiltrated into the gaps of the two-dimensional braid. The polymer solution formed to the surface separation layer and the interface layer after been immersed into a coagulation bath, which increased the friction between the filaments. And the embedded polymer within the gaps

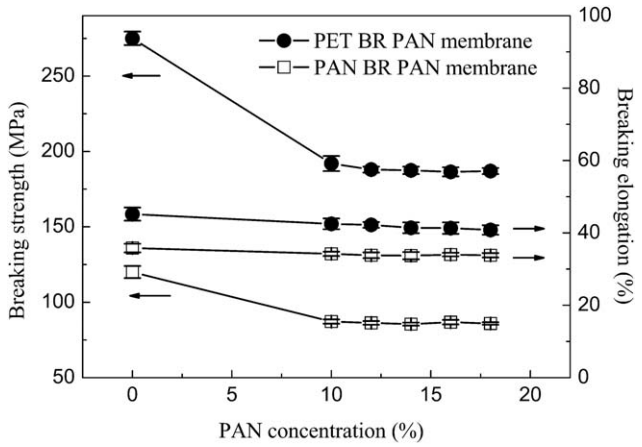

Figure 4. The breaking strength and breaking elongation of reinforced hollow fiber membranes with PAN concentration.

hindered deformation of the rhombus structure and the filaments gaps. Thus the yield strength, young's modulus, breaking strength and breaking elongation of the BR hollow fiber membrane were smaller than that of the two-dimensional braid as shown in Figure 3 and Table III.

Figure 4 shows the breaking strength and breaking elongation of the reinforced hollow fiber membranes with PAN concentration. Figure 4 displays that the breaking strength and breaking elongation of the PET or PAN BR hollow fiber membranes were similar under different PAN concentration. The tensile strength of the BR membranes was provided by the two-dimensional braid as the reinforcement matrix and the separating functional layer coated on the braid surface by interfacial bonding. But, compared with the two-dimensional braid, the contribution of separating functional layer and interfacial bonding to tensile strength of the BR membrane was minimal, because the separating functional layer and interfacial bonding layer had been broken prior to the broken of the two-dimensional braid. It indicated that the two-dimensional braid was the main provider of mechanical properties of the BR hollow fiber membranes, and the PAN coating layer was the separation functional layer of the BR PAN hollow fiber membranes.

We know that the tensile strength of PAN membranes prepared by the wet spinning method was almost 3 MPa.[3] A low tensile strength of PAN membrane might cause fiber breakage easily in the state of serviceability. The BR PAN hollow fiber membranes prepared by the BR method rather than that by the wet phase inversion method had excellent mechanical properties. The tensile strength of the BR PAN membranes was more than 80 MPa, which was adequate for MBR application. In fact, the slipping, peeling or breakage of the skin layer that was outside of the BR PAN hollow fiber membrane had occurred before the BR PAN hollow fiber membranes were broken. Thence, the separation performance of the BR PAN hollow fiber membranes might be deteriorative or lost. Therefore, the interfacial bonding state of the BR PAN membranes was rather important and should be further investigated.

Morphologies of PAN Hollow Fiber Membranes

Figure 5 displays the structure of the hollow fiber membranes prepared in different PAN concentrations (12, 14, and 16 wt %) of the polymer solutions by the BR method. Figure 5(a1–a3,b1–b3) shows the part cross-section structure and outer surface of the M12, M14, and M16 membranes, respectively. Figure 5(c1–c3,d1–d3) shows the part cross-section structure and outer surface of the N12, N14 and N16 membranes, respectively. The outer layer was the PAN coating layer, and the inner layer was

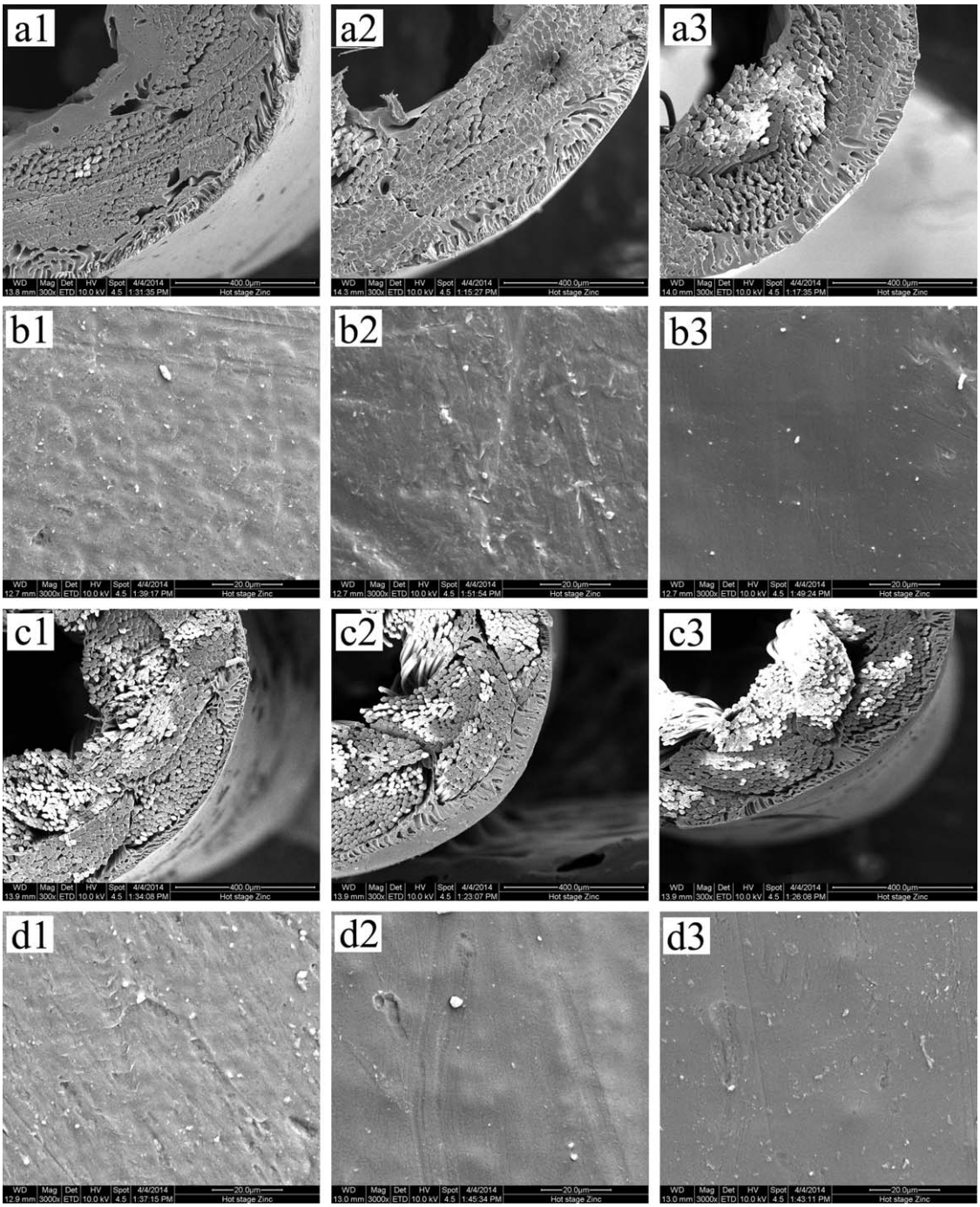

Figure 5. Cross-section and outer surfaces SEM morphologies of BR PAN hollow fiber membranes: (a1–a3) cross-section of (M12, M14, M16); (b1–b3) outer surface of (M12, M14, M16); (c1–c3) cross-section of (N12, N14, N16); (d1–d3) outer surface of (N12, N14, N16).

the two-dimensional braid. The middle layer, between the PAN coating layer and the two-dimensional braid, was the interface layer. Some of the coating solutions infiltrated into the gaps of the two-dimensional braid and formed a part of the interface layer, which endowed the BR hollow fiber membranes with high interfacial bonding. But, it can be seen that the extent of the polymer solutions embedded into the gaps of the PAN and PET two-dimensional braid were difference, the former was better than the later. That is because the PET two-dimensional braid and the PAN casting solutions were thermodynamic incompatibility, and DMAc was no co-solvent of them. Therefore, the PAN solutions had poor infiltrating into the PET two-dimensional braid. However, the PAN two-dimensional braid and the PAN casting solutions were thermodynamic compatibility and the DMAc in the PAN casting solutions was excellent co-solvent of them, so the PAN solutions had outstanding infiltrating into the gaps of PAN two-dimensional braid. Furthermore, the co-solvent could make the surface of the filaments

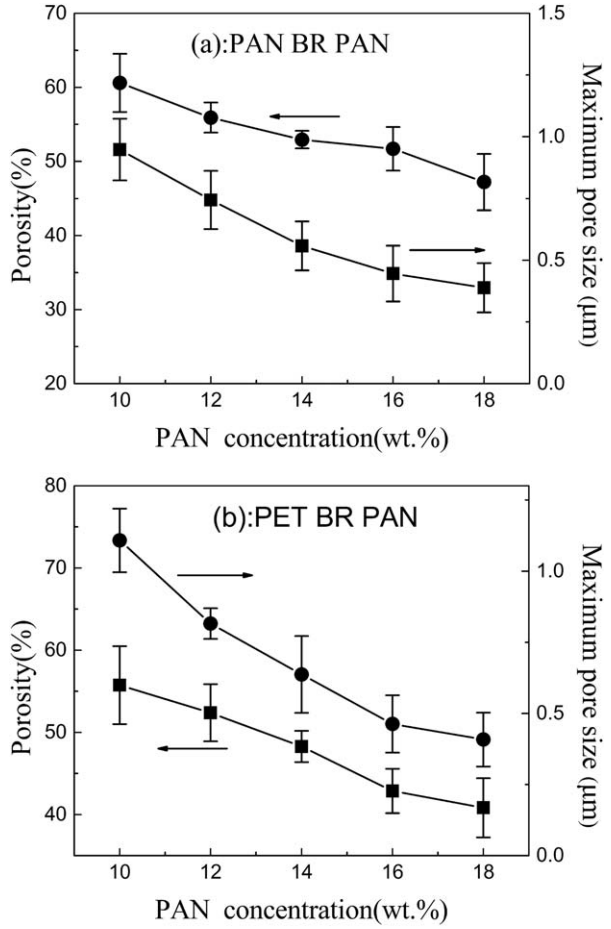

Figure 6. Effect of PAN concentration on the porosity and maximum pore size.

swelling or dissolving during the spinning process, and then enhanced the interfacial bonding state. The outer surface of the PAN and PET BR PAN hollow fiber membranes similarly appeared a dense layer, which thanked to the phase inversion process.

Permeation Properties of the PAN Hollow Fiber Membranes

Figure 6 shows the membrane porosity and maximum pore size of the PAN BR PAN and PET BR PAN hollow fiber membranes, respectively. The membrane porosity and maximum pore size had the same decreasing tendency as the increase of PAN concentration in the polymer solutions. It is well known that the increase of polymer concentration in the casting solution generally leaded to the increase of viscosity which decreased the porosity and the pore size of the membrane.[4] The porosity of the PAN BR PAN was lower than that of the PET BR PAN, because of the solvent of the PAN casting solutions was DMAc, in which the PAN two-dimensional braid dissolved excellently but PET two-dimensional braid did not dissolve. Thus, the casting solutions infiltrated into the gaps of PAN two-dimensional braid more than that of the PET two-dimensional braid in the spinning process. Both the PAN BR PAN and PET BR PAN hollow fiber membranes had a denser outer surface, as shown in Figure 5. These meant that the BR PAN hollow fiber membranes possessed a smaller maximum pore size which could improve the rejection of the membrane.

Figure 7 shows the PWF and protein rejection of the prepared PAN hollow fiber membranes. According to Figure 7, the PWF of the PAN BR PAN and the PET BR PAN hollow fiber membranes decreased slightly from 344.3 L m^{-2} h^{-1} for the M10 to 87.4 L m^{-2} h^{-1} for the M18 and from 467.2 L m^{-2} h^{-1} for the N10 to 105.1 L m^{-2} h^{-1} for the N18, with the increase of PAN concentration from 10 to 18 wt %. But the rejection ratio increased with the increase of PAN concentration. The BR PAN hollow fiber membranes had a thick outer wall, which extended the membrane filtration path and increased the intrinsic resistance of the membrane. Therefore, with the increase of PAN concentration in the polymer solutions, the wall thickness became thicker and the PWF of the BR PAN hollow fiber membranes became lower. The outer wall of the PET BR PAN hollow fiber membranes were thinner than the PAN BR PAN, showed in Figure 5. Moreover, the pore size was a key factor impacting the membrane permeability, the maximum pore size decreased with the increase of PAN concentration in polymer solution from Figure 6. The rejection depended more on the denseness of the skin layer than on the structure of the cross-section.[26] Therefore, the PWF of the PAN BR PAN hollow fiber membrane was greater than that of the PET BR PAN prepared

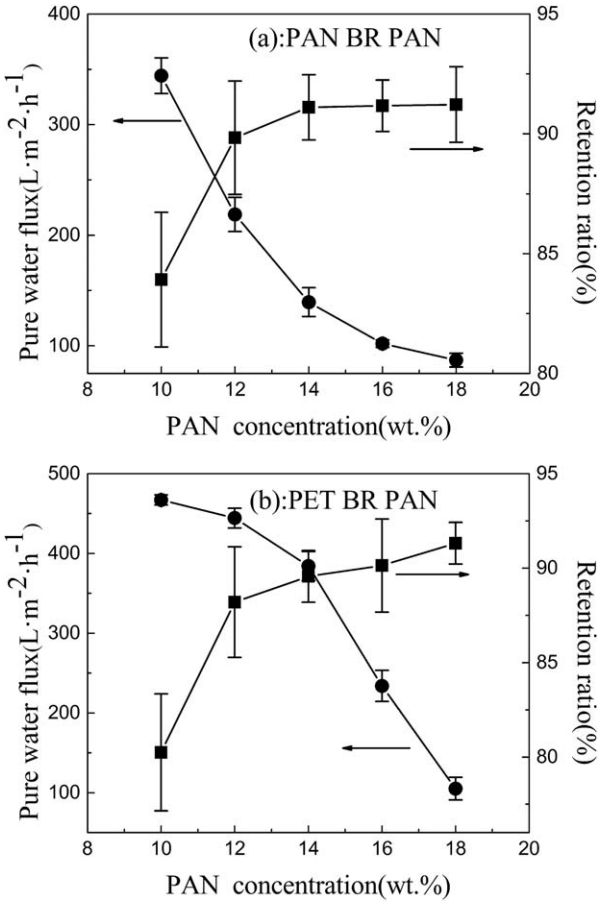

Figure 7. Effect of the PAN concentration on pure water flux and protein rejection of the membranes.

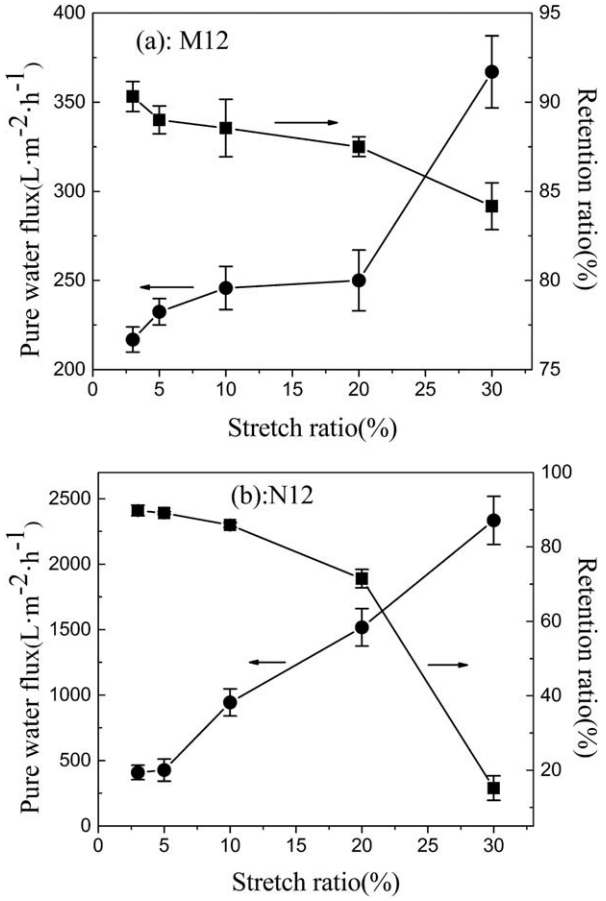

Figure 8. Effect of the stretch ratio on pure water flux and protein rejection of the PAN membranes.

with the same casting solution and the protein rejections of them were similar.

The skin layers of the BR PAN hollow fiber membrane were dense and the maximum pore size of the BR PAN hollow fiber membranes were small. Thus, with the application of the BR method, the increasing rate of the protein separation was significant for some special water treatment.

Interfacial Bonding State of the Hollow Fiber Membranes

The PWF and protein rejection of the prepared M12 and N12 hollow fiber membranes were shown in Figure 8, which stretched at the constant speed of 20 mm min^{-1}. According to Figure 8, the PWF of the PAN BR PAN and the PET BR PAN hollow fiber membranes increased after stretching process. In additional, the rejection ratios of them were reduced with the increase of stretch ratio. The PWF and protein rejection of the prepared PET BR PAN hollow fiber membranes had small change amplitude under the stretch ratio of 5%, afterward, the PWF increased rapidly and the protein rejection decreased quickly with the increase of stretch ratio. However, the PWF and protein rejection of the prepared PAN BR PAN hollow fiber membranes had small change amplitude below the stretch ratio of 20%, subsequently, the change amplitude of the PWF and protein rejection increased sharply. The interface between the surface separation layer and the two-dimensional braided tube was damaged during the stretching process. Even worse, the surface separation layer had been broken which leaded to lose the membranes separating performance. It indicated that the interfacial bonding state of PAN BR PAN hollow fiber membranes was better than that of PET BR PAN hollow fiber membranes.

Figure 9 shows the cross-section and outer surface SEM morphologies of stretched M12 and N12 hollow fiber membranes. The cross-section SEM morphologies of M12 were changed inconspicuously after stretching process, as shown in Figure 9(a). The outer surface SEM morphologies of M12 were piecemeal deformation with the stretch ratio increasing, but the surface separation layers were not broken as shown in Figure 9(b). This was due to the DMAc was the favorable co-solvent of the PAN casting solutions and the PAN two-dimensional braid. Thus, the PAN solutions had wonderful infiltrating into the gaps of the PAN two-dimensional braid. The DMAc of the immersed casting solutions could make the surface of the filaments swelling or dissolving during the spinning process. After being immersed in the coagulation bath, the immersed casting solutions formed a part of the prepared PAN hollow membrane and enhanced the interfacial bonding state. The interface was not only mechanical bonding but also chemical bonding. Therefore, the PAN surface separating layer and the PAN two-dimensional braid deformed simultaneously during stretching. Obviously, the cross-sectional and the outer surface SEM morphologies of N12 were different from M12. It can be seen from Figure 9(c,d), the interface between the PAN surface separating layer and the PET two-dimensional braid tube was gradually destroyed and the PAN surface separating layer was peeled off from PET two-dimensional braid tube with the increase of stretch ratio. The interface between PAN surface separating layers and the PET two-dimensional braid damaged increasingly with the increase of stretch ratio, until it became delamination from the PET two-dimensional braid. Then, the PET BR PAN hollow fiber membrane lost its separation properties. This could be proved from Figure 8(b), the PWF increased rapidly and the protein rejection decreased quickly with the stretch ratio increasing. Because of the PAN casting solutions and the PET two-dimensional braid were thermodynamic incompatibility and the DMAc was not the co-solvent of them, the PAN solutions have poor infiltrating into the gaps of PET two-dimensional braid. And the interface was mechanical bonding rather than chemical bonding. The results confirmed that the interfacial bonding state of the PAN two-dimensional braided tube reinforced homogeneous PAN hollow fiber membranes was better than that of the PET two-dimensional braided tube reinforced heterogeneous.

CONCLUSIONS

The homogeneous and heterogeneous BR PAN hollow fiber membranes were prepared through the dry–wet spinning method which coated PAN polymer solutions on the PAN and PET two-dimensional braid surface, respectively. The BR PAN hollow fiber membranes prepared by the BR method had outstanding mechanical properties and its tensile strength was higher than 80 MPa, which was adequate for special applications. The BR PAN hollow fiber membranes had a favorable interfacial bonding

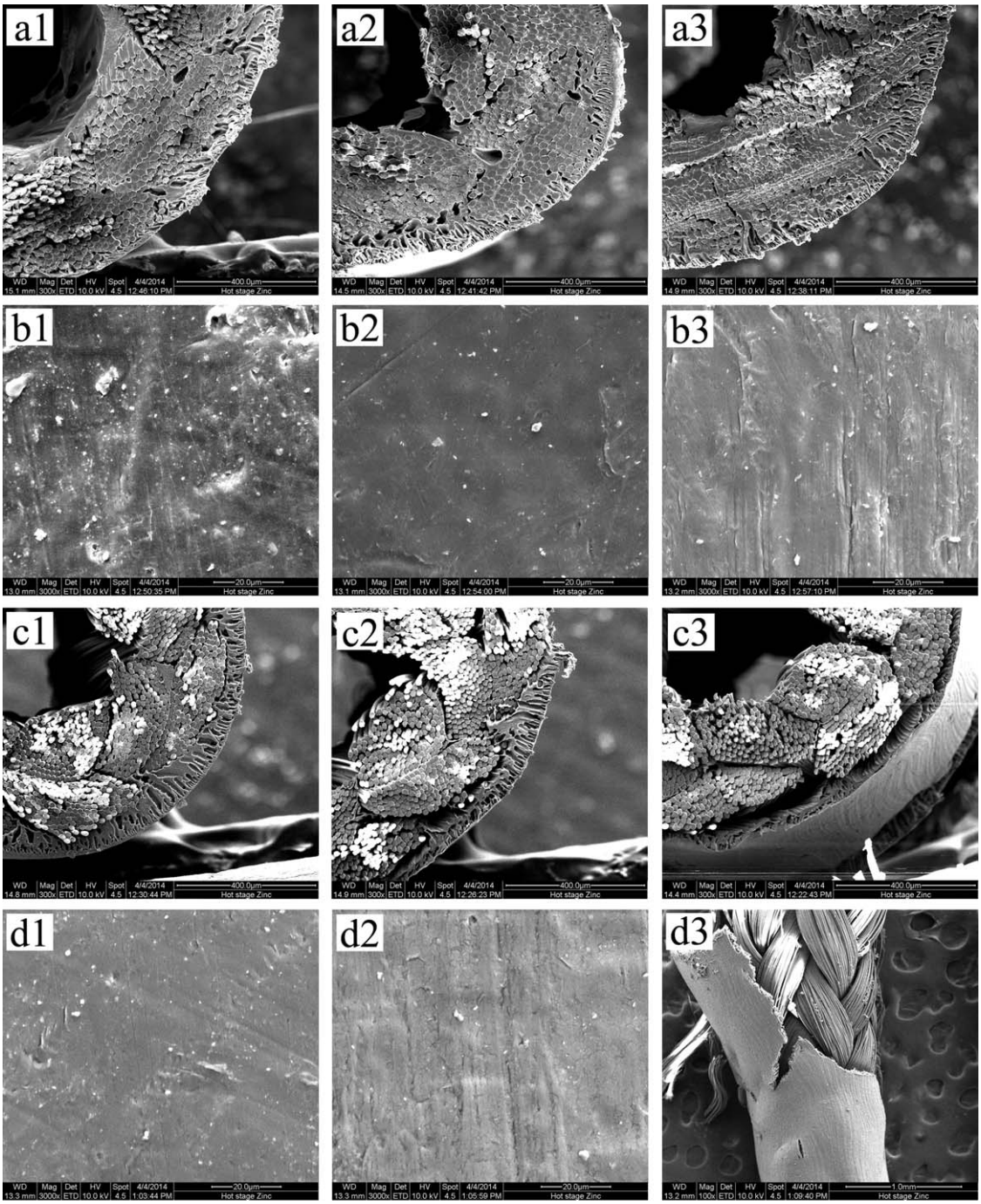

Figure 9. Cross-section and outer surface SEM morphologies of stretched braided tube reinforced PAN hollow fiber membranes: (a1–a3) M12 cross-section, stretch ratio: 3%, 10%, 30%; (b1–b3) M12 outer surface, stretch ratio: 3%, 10%, 30%; (c1–c3) N12 cross-section, stretch ratio: 3%, 10%, 30%; (d1–d3) N12 outer surface, stretch ratio: 3%, 10%, 30%.

between the coating layer and two-dimensional braid due to the existence of the interface layer. The outer surface of the BR PAN hollow fiber membrane was a dense layer as the separating functional layer. The maximum pore size of the BR PAN hollow fiber membranes decreased with the increase of PAN concentration, which could result in lower PWF and higher rejection of protein. The interfacial bonding state of the PAN two-dimensional braided tube reinforced homogeneous PAN hollow fiber membranes was better than the PET two-dimensional braided tube reinforced heterogeneous PAN hollow fiber membranes.

ACKNOWLEDGMENTS

The authors gratefully acknowledge the research funding provided by the 973 Program (2012CB722706) of China, the 863 Program (2012AA03A603) of China, the National Natural Science

Foundation of China (21274109), and the PCSIRT of Ministry of Education of China (IRT13084).

REFERENCES

1. Khayet, M.; Feng, C. Y.; Khulbe, K. C.; Matsuura, T. *Polymer* **2002**, *43*, 3879.
2. Nouzaki, K.; Nagata, M.; Arai, J.; Idemoto, Y.; Koura, N.; Yanagishita, H.; Negishi, H.; Kitamoto, D.; Ikegami, T.; Haraya, K. *Desalination* **2002**, *144*, 53.
3. Scharnagl, N.; Buschatz, H. *Desalination* **2000**, *139*, 191.
4. Feng, C.; Wang, R.; Shi, B.; Li, G.; Wu, Y. *J. Membr. Sci.* **2006**, *277*, 55.
5. Jung, B. *J. Membr. Sci.* **2004**, *229*, 129.
6. Chaturvedi, B.; Ghosh, A.; Ramachandhran, V.; Trivedi, M.; Hanra, M.; Misra, B. *Desalination* **2001**, *133*, 31.
7. Lee, H.; Won, J.; Lee, H.; Kang, Y. *J. Membr. Sci.* **2002**, *196*, 267.
8. Yuliwati, E.; Ismail, A. F. *Desalination* **2011**, *273*, 226.
9. Qin, J. J.; Cao, Y. M.; Li, Y. Q.; Li, Y.; Oo, M. H.; Lee, H. *Sep. Purif. Technol.* **2004**, *36*, 149.
10. Patsios, S. I.; Karabelas, A. J. *J. Membr. Sci.* **2011**, *372*, 102.
11. Judd, S. The MBR Book: Principles and Applications of Membrane Bioreactors in Water and Wastewater Treatment; Elsevier: London, **2006**; Chapter 2, p 54.
12. Kim, M. J.; Sankararao, B.; Yoo, C. K. *J. Membr. Sci.* **2011**, *375*, 345.
13. Murase, K.; Habara, H.; Fujiki, H.; Hirane, T.; Mizuta, M. US Patent 2002/0046970A1, **2002**.
14. Meng, F.; Chae, S. R.; Drews, A.; Kraume, M.; Shin, H.-S.; Yang, F. *Water Res.* **2009**, *43*, 1489.
15. Lee, M. S.; Choi, S. H.; Shin, Y. C. US Patent 7267872, **2007**.
16. Liu, J.; Li, P. L.; Xie, L. X.; Wang, S. C.; Wang, Z. *Desalination* **2009**, *249*, 453.
17. Zhang, X. L.; Xiao, C. F.; Hu, X. Y.; Bai, Q. Q. *Appl. Surf. Sci.* **2013**, *264*, 801.
18. Yang, S.; Liu, Z. Z. *J. Membr. Sci.* **2003**, *222*, 87.
19. Asatekin, A.; Olivetti, E. A.; Mayes, A. M. *J. Membr. Sci.* **2009**, *332*, 6.
20. Tsai, H. A.; Ye, Y. L.; Lee, K. R.; Huang, S. H.; Suen, M. C.; Lai, J. Y. *J. Membr. Sci.* **2011**, *368*, 254.
21. Guedidi, S.; Yurekli, Y.; Deratani, A.; Dejardin, P.; Innocent, C.; Altinkaya, S. A.; Roudesli, S.; Yemenicioglu, A. *J. Membr. Sci.* **2010**, *365*, 59.
22. Wang, Z. G.; Wan, L. S.; Xu, Z. K. *J. Membr. Sci.* **2007**, *304*, 8.
23. Wang, H.; Zhang, Q.; Zhang,S. *J. Membr. Sci.* **2011**, *378*, 243.
24. Liu, G.; Yang, D.; Zhu, Y.; Ma, J.; Nie, M.; Jiang, Z. *Chem. Eng. Sci.* **2011**, *66*, 4221.
25. Packham, D. E. *Int. J. Adhes. Adhes.* **1986**, *6*, 225.
26. Amirilargani, M.; Mohammadi, T. *Polym. Adv. Technol.* **2009**, *20*, 993.